What Makes Red Visual Pigments Red? A Resonance Raman Microprobe Study of Retinal Chromophore Structure in Iodopsin†

Steven W. Lin,‡,§ Yasushi Imamoto,‖ Yoshitaka Fukada,‖,⊥ Yoshinori Shichida,‖ Tôru Yoshizawa,# and Richard A. Mathies*,‡

Department of Chemistry, University of California, Berkeley, California 94720, Department of Biophysics, Faculty of Science, Kyoto University, Kitashirakawa-oiwake-cho, Sakyo-ku, Kyoto 606, Japan, and Department of Information System Engineering, Faculty of Engineering, Osaka Sangyo University, Daito-shi, Osaka 574, Japan

Received October 6, 1993; Revised Manuscript Received December 1, 1993⊛

ABSTRACT: We have obtained resonance Raman spectra of iodopsin, a red-sensitive (λ_{max} 571 nm) pigment from chicken cone cells, to investigate the molecular mechanism of the opsin shift in visual pigments. Detergent-solubilized iodopsin samples were examined with a Raman microprobe to obtain spectra from a 77-K photostationary steady-state mixture composed of 11-*cis*-iodopsin and its 9-*cis*-isoiodopsin and *all-trans*-bathoiodopsin photoproducts. The vibrational modes of these species have been assigned by comparison with spectra of the corresponding bovine pigments. The single bond stretching frequencies of the bovine, toad, and chicken pigments are found to exhibit a regular correlation as a function of the pigment absorption maxima that is consistent with the expected effects of increased electron delocalization. The C=NH stretching frequencies of iodopsin and bathoiodopsin are at 1644 and 1638 cm^{-1}, respectively, and shift down to 1621 and 1617 cm^{-1}, respectively, when the nitrogen is deuterated. The C=ND stretching frequencies of the various pigments are found to decrease linearly with increasing absorption maxima, suggesting that at least part of the opsin shift in visual pigments results from weakened electrostatic interaction between the retinal chromophore and its protein counterion. The Raman data are inconsistent with the idea that a charged protein residue is shifted along the chromophore to regulate the opsin shift. Taken together with the mutagenesis and model compound results, these resonance Raman data suggest that the opsin shift between the green and red cone visual pigments arises from two effects. First, Tyr-274 provides increased electrostatic stabilization of the Schiff base–counterion ion pair. Second, the opsin shift is enhanced by the dipolar residues Ser-177 and Thr-282 that interact with the chromophore near the ionone ring to preferentially stabilize the highly dipolar charge distribution of the electronically excited retinal chromophore [Mathies, R., & Stryer, L. (1976) *Proc. Natl. Acad. Sci. U.S.A. 73,* 2169–2173].

Color vision in vertebrates is mediated by three visual pigments in the cone cells of the retina that absorb maximally in the blue (~430 nm), green (~530 nm) , and red (~560 nm) regions of the spectrum (Lythgoe, 1972; Yoshizawa, 1992). Rod cells which are responsible for dim-light, black-and-white vision contain rhodopsin absorbing maximally at 500 nm. All visual pigments consist of an 11-*cis*-retinal chromophore that is covalently linked by a protonated Schiff base (PSB)[1] bond to a conserved lysine residue on a ~40 000-Da intrinsic membrane protein called opsin. Although protonated retinal Schiff bases absorb maximally at ~440 nm in organic solvents, unique chromophore–protein interactions in each pigment induce an opsin shift of the absorption maximum (λ_{max}) of the chromophore over a 130-nm range (Nakanishi et al., 1980). The λ_{max} of protonated retinal Schiff bases can be modulated (1) by changing the separation between the PSB group and its counterion (Blatz et al., 1972), (2) by placing charged or dipolar groups along the polyene (Honig et al., 1979), (3) by changing the dielectric properties of the environment (Irving et al., 1970), or (4) by changing the conformation about the C_6–C_7 single bond (Harbison et al., 1985; Honig et al., 1976; van der Steen et al., 1986). Understanding the origin of the opsin shift in visual pigments is one of the fundamental goals of vision research.

The chromophore structure and environment in bovine rhodopsin have been studied extensively to elucidate its opsin-shift mechanism. An external point-charge perturbation near C_{12} was first proposed on the basis of dihydroretinal analog studies (Honig et al., 1979; Nakanishi et al., 1980). However, site-specific mutagenesis has shown that no charged residue exists in the protein interior besides the Glu-113 counterion (Nathans, 1990b; Sakmar et al., 1989; Zhukovsky & Oprian, 1989). The resonance Raman spectrum of rhodopsin reveals a high Schiff base stretching frequency that has been interpreted in terms of a strong hydrogen-bonding interaction between the PSB group and its counterion (Deng & Callender, 1987; Eyring & Mathies, 1979; Mathies et al., 1976; Palings et al., 1987). Solid-state ^{13}C-NMR experiments demonstrate that the C_6–C_7 single bond conformation is *s-cis* (Smith et al.,

† This research was supported by the National Institutes of Health (Grant EY 02051 to R.A.M.) and in part by Grants-in-Aid for Scientific Research and Cooperative Research from the Japanese Ministry of Education, Culture and Science, by a Human Frontier Science Program, and by a Grant-in-Aid for JSPS fellows.

* Author to whom correspondence should be addressed.

‡ University of California, Berkeley.

§ This work constitutes a portion of the Ph.D. Thesis of S.W.L. in the Graduate Group in Biophysics.

‖ Kyoto University.

⊥ Present address: Department of Pure and Applied Sciences, College of Arts and Sciences, The University of Tokyo, Komaba, Meguro, Tokyo 153, Japan.

Osaka Sangyo University.

⊛ Abstract published in *Advance ACS Abstracts,* February 1, 1994.

[1] Abbreviations: HEPES, *N*-(2-hydroxyethyl)piperazine-*N'*-2-ethanesulfonic acid; CHAPS, 3-[(3-cholamidopropyl)dimethylammonio]-1-propanesulfonate; PC, L-α-phosphatidylcholine; ConA, concanavalin A; PSB, protonated Schiff base; BR_{568}, light-adapted bacteriorhodopsin.

0006-2960/94/0433-2151$04.50/0

1987a) and that there is unusual deshielding along the chain between the C_8 and C_{13} positions (Smith et al., 1990). The electron distribution derived from the NMR spectra has been used to constrain the location of the carboxylate counterion near the C_{12} region of the polyene (Han et al., 1993), in general agreement with the model of the chromophore–counterion complex proposed by Birge and co-workers on the basis of two-photon absorption studies (Birge et al., 1985, 1988). Recent model studies suggest that the NMR and vibrational data may be modeled by a retinal PSB molecule in an environment where the Schiff base is not interacting directly with the counterion and is hydrogen-bonded to a separate dipolar group (Albeck et al., 1992; Livnah & Sheves, 1993).

A comparative study of the chromophore structures in visual pigments with absorption maxima between 430 and 500 nm was first carried out by Barry and Mathies (1987) using resonance Raman microprobe spectroscopy. A subsequent study by Loppnow et al. (1989) examined the Raman spectra of the green rod (λ_{max} ~433 nm) and red rod (λ_{max} 502 nm) pigments from the toad *Bufo marinus* to elucidate the structural basis of the opsin shift in a color visual pigment. These spectra showed that the chromophore in the blue pigment was a *protonated* retinal Schiff base residing in an environment lacking any specific protein perturbations. Since no spectra of red-absorbing visual pigments were available, an examination of the mechanism of larger opsin shifts was not possible.

Iodopsin is the visual pigment in the red cone cells of the chicken retina (Yoshizawa & Kuwata, 1991). Its sequence is 80% identical to that of the human red cone pigment (λ_{max} 560 nm), and according to the structural model of rhodopsin and G-protein-coupled receptors proposed by Baldwin (1993), none of the differences involve residues on helices 3, 6, and 7 that form the binding pocket for the chromophore. Therefore, iodopsin can serve as a model system for vertebrate red-sensitive cone pigments. The photochemistry of iodopsin has been characterized by low-temperature absorption spectroscopy (Hubbard & Kropf, 1959; Yoshizawa & Wald, 1967), and at room temperature with picosecond (Kandori et al., 1990) and nanosecond (Shichida et al., 1993) time resolution. The absorption maxima of iodopsin (Imamoto et al., 1989) and the human red cone pigment (Wang et al., 1993) shift to the blue by ~1000 cm^{-1} in the absence of chloride ions, and this appears to be a general characteristic of red cone pigments (Kleinschmidt & Harosi, 1992). Mutagenesis experiments on the human pigment have indicated that His-197 and Lys-200, located on the exterior loop connecting helices 3 and 4, form the chloride binding site. Studies of the chromophore binding pocket structure in iodopsin using retinal analogs have suggested that the opsin shift is caused by weak hydrogen bonding of the Schiff base with its counterion and by the presence of a negative charge perturbation near C_{13} (Fukada et al., 1990) or C_7 (Chen et al., 1989). Analog experiments on the green and red cone pigments from salamander, squirrel, and monkey are consistent with a twisted *s-cis* conformation for the C_6–C_7 bond for both pigments, indicating that the opsin shift in the red pigment is not caused by a change of the C_6–C_7 bond conformation (Makino et al., 1990). In the work presented here, we extend the comparison of retinal chromophore structures using resonance Raman spectroscopy to iodopsin and examine the differences in chromophore–protein interactions between the blue-, green-, and red-sensitive pigments with the goal of understanding the physical mechanisms responsible for the opsin shift in the red-sensitive cone pigments.

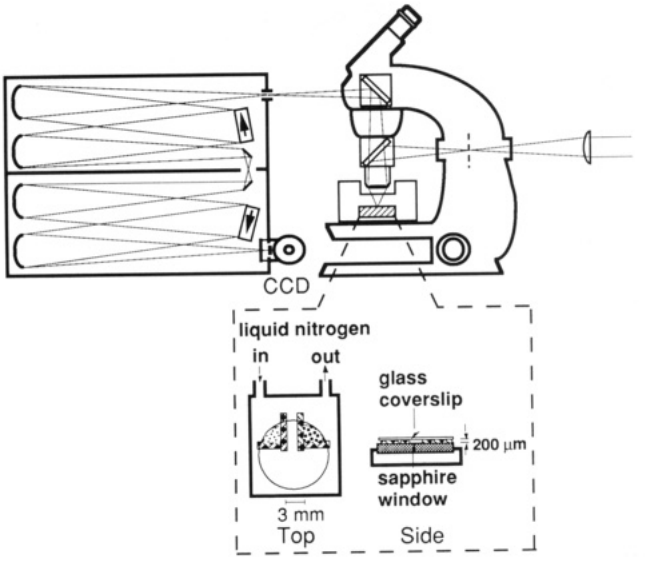

FIGURE 1: Raman microprobe system. Emission from a Kr^+ laser and/or a Ti:sapphire laser pumped by the all-lines output from an Ar^+ laser is focused on the sample by a 40× long-working-length objective lens. Backscattered light collected by the objective lens is coupled into the spectrograph, dispersed, and focused onto the liquid-nitrogen-cooled CCD detector. The pigment and its bleached blank are frozen on separate quadrants of a sapphire window in a specially constructed 77-K cold stage (Loppnow & Mathies, 1989). Details of the sample loading procedure and detection apparatus are described in Lin et al. (1992).

MATERIALS AND METHODS

Iodopsin was prepared according to the method of Okano et al. (1989). The outer segments of rods and cones were isolated from 1500 chicken retinas by flotation in standard buffer (SB) (50 mM HEPES, 140 mM NaCl, 1 mM dithiothreitol, 0.1 mM phenylmethanesulfonyl fluoride, 4 μg/mL leupeptin, and 60 kallikrein inhibitor units/mL aprotinin, pH 6.6) containing 40% (w/v) sucrose. After being washed with SB, the visual pigments were solubilized by SB supplemented with 0.75% CHAPS, 1.0 mg/mL PC, 1 mM $MnCl_2$, and 1 mM $CaCl_2$. The extract was diluted by the addition of 0.25 volume of SB and then applied to a ConA–Sepharose affinity chromatography column. Oil droplets and impurities were removed by washing the column with a detergent buffer (SB supplemented with 0.6% CHAPS and 0.8 mg/mL PC, 1 mM $MnCl_2$, and 1 mM $CaCl_2$). Iodopsin was then eluted with detergent buffer supplemented with 1.5 mM methyl α-mannoside. Fractions containing mostly iodopsin (absorbance of 0.05/cm at 571 nm) were collected and concentrated by ultrafiltration (YM-30, Amicon). After removal of methyl α-mannoside by dialysis against a detergent buffer, iodopsin was adsorbed to a ConA column and eluted by detergent buffer supplemented with 100 mM methyl α-mannoside. The absorbance at 571 nm was about 1.0/cm. The exchangeable protons of the pigment were deuterated by dialyzing a portion of the original iodopsin sample against a D_2O buffer (50 mM HEPES, 140 mM NaCl, 0.75% CHAPS, and 1.0 mg/mL PC, pH 6.6) for 2 days.

Resonance Raman spectroscopy was performed using the Raman microprobe illustrated in Figure 1 (Lin et al., 1992; Loppnow & Mathies, 1989). Probe light (530.9 nm) from a Kr^+ laser (Spectra-Physics 2025) and 710- or 750-nm pump light from a Ti:sapphire laser (Lexel 479), pumped by the all-lines output from an Ar^+ laser (Spectra-Physics 2020), were focused by a 40× objective to an ~100 × 5 μm area on the sample. Backscattered Raman light was dispersed in a double spectrograph (Mathies & Yu, 1978) and detected by

a cryogenically cooled CCD detector (LN/CCD-1152, Princeton Intruments) controlled by a ST-130 controller (Princeton Instruments). Iodopsin (2 μL) with a maximum absorbance of ~1.6/cm at 571 nm and an equal volume of its bleached solution were pipetted into adjacent microcells inside the cold stage and frozen to 77 K following the procedures in Lin et al. (1992). The fluorescence background was removed by subtracting the bleached-pigment spectrum from the iodopsin spectrum. Frequencies were assigned using atomic emission lines from an iron hollow cathode lamp to calculate wavelength dispersion across the detector face. The reported frequencies are accurate within 3 cm^{-1}, and the spectral resolution is 6 cm^{-1}.

RESULTS

Characterization of the 77-K Photostationary Mixture. The photochemistry of iodopsin at 77 K was first examined by Yoshizawa and Wald (1967). Irradiation of iodopsin with green (~500 nm) light creates a mixture consisting of 11-*cis*-iodopsin (λ_{max} 571 nm) and its photoproducts 9-*cis*-isoiodopsin (λ_{max} 550 nm) and *all-trans*-bathoiodopsin (λ_{max} 640 nm), which is analogous to the 77-K mixture established in bovine rhodopsin (Yoshizawa & Wald, 1963). However, in the iodopsin steady-state mixture, less of the 9-*cis* isomer is produced. Irradiation of the 77-K mixture with red light (>640 nm) converts bathoiodopsin preferentially to iodopsin. Photoconversion between iodopsin and bathoiodopsin occurs with an isosbestic point at 595 nm, indicating that only a small amount of isoiodopsin is present in the mixture.

The resonance Raman spectra of iodopsin at 77 K obtained with a probe wavelength of 530.9 nm are presented in Figure 2. Irradiation of the sample with green light creates a mixture that contains predominantly iodopsin and bathoiodopsin. In the probe-only spectrum, two intense bands at 1502 and 1527 cm^{-1} are detected in the ethylenic (C=C) region (Figure 2A). The 1502-cm^{-1} line is assigned to the C=C stretch of bathoiodopsin because it disappears when the red pump beam is added (Figure 2B), and also because its C=C stretching mode must have the lowest frequency on the basis of the inverse correlation between the λ_{max} of retinals and their C=C frequencies (Barry & Mathies, 1987; Doukas et al., 1978; Rimai et al., 1973). The band at 1527 cm^{-1} is assigned to the in-phase C=C stretch of iodopsin because it is expected to be the other major component in the mixture (Tsukamoto et al., 1975; Yoshizawa & Wald, 1967). The 1527-cm^{-1} frequency is also close to that expected for iodopsin based on the above-mentioned correlation. Moreover, modes belonging to 9-*cis*-isoiodopsin are also detected in the probe-only spectrum. Lines at ~1154 and ~1322 cm^{-1} which are characteristic of 9-*cis*-retinals (Curry et al., 1985) are present. The C=C mode of isoiodopsin is expected to lie near ~1530 cm^{-1} on the basis of its 550-nm λ_{max} (Yoshizawa & Wald, 1967), and most likely cannot be resolved from the broad iodopsin band at 1527 cm^{-1}. Although the amount of isoiodopsin in the mixture is expected to be small, its Raman lines are detected because the 530.9-nm probe wavelength is close to the λ_{max} of isoiodopsin.

The composition of the steady-state mixture was altered by adding 710- or 750-nm pump illumination. The red light converts bathoiodopsin mostly back to iodopsin as seen by the increase in the height of the 1527-cm^{-1} band and the decrease of the 1502-cm^{-1} band (Figure 2B). The pump+probe spectrum also contains nearly the same relative proportion of isoiodopsin scattering based on the similar intensities of the

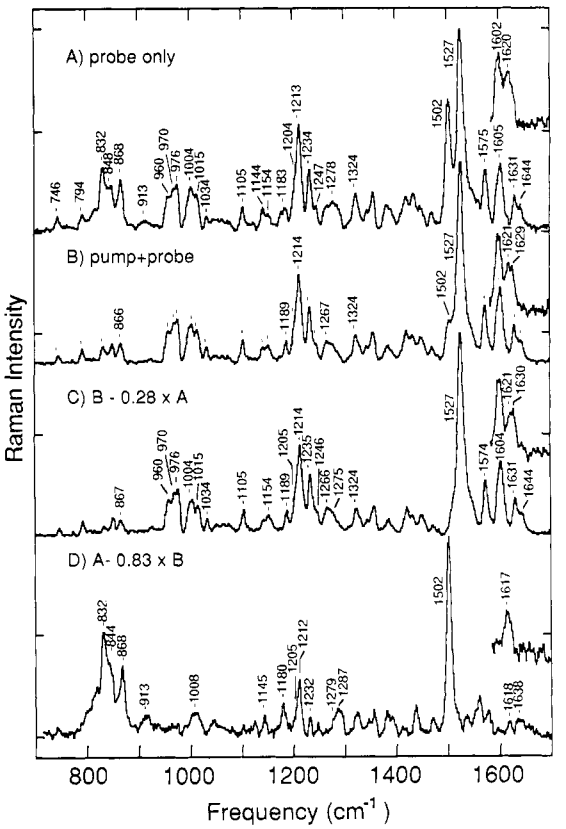

FIGURE 2: Resonance Raman microprobe spectra of iodopsin frozen at 77 K obtained (A) with 530.9-nm probe (~5 mW) excitation and (B) with 530.9-nm probe (~1 mW) and 750-nm pump (~20 mW) excitations. (C) Spectrum of the iodopsin+isoiodopsin mixture and (D) spectrum of bathoiodopsin calculated from the difference of (A) and (B). The inset in each spectrum presents the Schiff base region obtained from samples in D_2O buffer.

1154- and 1324-cm^{-1} lines in the probe-only and pump+probe spectra. In addition, a singular-value decomposition analysis of a set of spectra obtained with varying pump-to-probe power ratios showed that the data are composed of two basis spectra. These results indicate that the relative proportion of Raman scattering from iodopsin and isoiodopsin stays nearly constant under our experimental conditions and, therefore, the Raman spectra can be represented as a linear combination of the bathoiodopsin and iodopsin+isoiodopsin spectra. A pure spectrum of bathoiodopsin was obtained by subtracting a fraction of the pump+probe spectrum from the probe-only spectrum until the 1527-cm^{-1} line was removed (Figure 2D). Similarly, subtracting the small bathoiodopsin contribution from the pump+probe spectrum generates a Raman spectrum of the iodopsin+isoiodopsin mixture (Figure 2C).

Iodopsin and Isoiodopsin. The 9-*cis* and 11-*cis* isomers of retinal can be distinguished by the characteristic patterns of their vibrational lines (Curry et al., 1985; Palings et al., 1987). The assignments of bands to either iodopsin or isoiodopsin in the mixture (Figure 2C) and the determination of their normal mode character can be made by comparison with the Raman spectra of bovine rhodopsin (11-*cis*) and isorhodopsin (9-*cis*). The vibrational character of modes in the Raman spectra of rhodopsin and isorhodopsin (Figure 3) has been assigned by Palings et al. (1987). In rhodopsin, the C_{10}–C_{11}, C_{14}–C_{15}, C_8–C_9, and C_{12}–C_{13} stretching modes are found at 1098, 1190, 1217, and 1239 cm^{-1}, respectively. The low frequency of the C_{10}–C_{11} stretch is due to the *cis* configuration of the adjacent C_{11}=C_{12} bond. The C_8–C_9 and C_{12}–C_{13} stretching modes have higher frequencies due to coupling with the adjacent

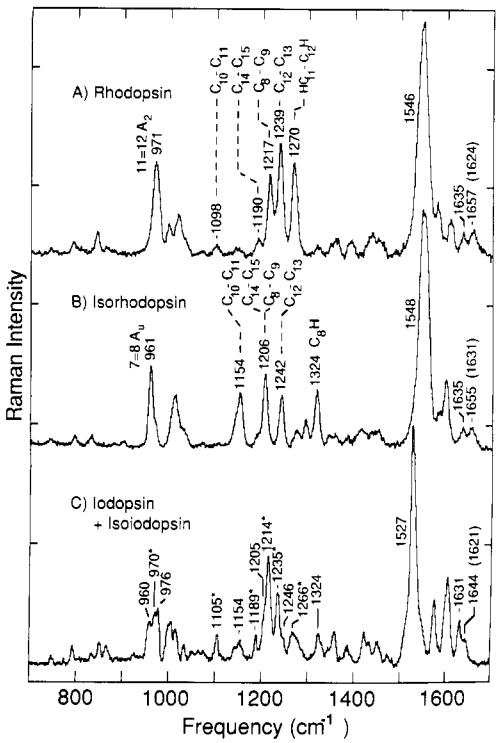

FIGURE 3: Resonance Raman spectra of (A) rhodopsin, (B) isorhodopsin, and (C) iodopsin+isoiodopsin mixture from Figure 2C. Rhodopsin and isorhodopsin spectra were obtained by exciting flowing solutions of bovine pigments at room temperature with a 488.0-nm probe beam. The vibrational assignments for rhodopsin and isorhodopsin are from Palings et al. (1987). Lines assigned to iodopsin are labeled with an asterisk. The deuterated Schiff base frequencies are indicated in parentheses.

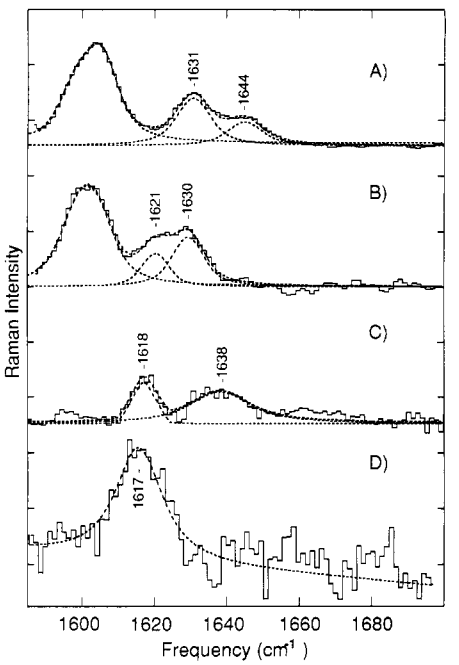

FIGURE 4: Schiff base region of the Raman spectrum of the iodopsin+isoiodopsin mixture in (A) H_2O and (B) D_2O at 77 K. Spectrum of bathoiodopsin in (C) H_2O and (D) D_2O at 77 K. Bands were least-squares-fit to a sum of Lorentzian bandshapes. The bathoiodopsin spectra taken in H_2O and D_2O buffers were scaled using the intensities of the HOOP and fingerprint lines.

methyl stretches. In isorhodopsin, the C_{10}–C_{11} stretch is also found at a lower frequency (1154 cm^{-1}) because the C_{10}–C_{11} bond is next to the C_9=C_{10} *cis* linkage. This mode has substantial Raman intensity and serves as a marker band for the 9-*cis* isomer (Curry et al., 1985). The C_{14}–C_{15} and C_8–C_9 stretches of isorhodopsin are degenerate at ~1206 cm^{-1}, and the C_{12}–C_{13} stretch appears at 1242 cm^{-1}.

The Raman spectrum of the mixture containing iodopsin and isoiodopsin is compared with spectra of bovine rhodopsin and isorhodopsin in Figure 3. Lines are found in the iodopsin spectrum whose frequencies correspond well with those of rhodopsin and isorhodopsin except for differences in their relative intensities. Thus, the C–C modes in the iodopsin spectrum have been assigned by correspondence with the rhodopsin and isorhodopsin spectra. The C_{10}–C_{11} stretch of iodopsin is assigned at 1105 cm^{-1}. The C_{14}–C_{15}, C_8–C_9, and C_{12}–C_{13} modes of iodopsin are assigned at 1189, 1214, and 1235 cm^{-1}, respectively. The line at 1154 cm^{-1} is assigned to the C_{10}–C_{11} stretch of isoiodopsin because this band is unique to the 9-*cis* isomer. The shoulder at 1246 cm^{-1}, with roughly the same peak height as the 1154-cm^{-1} band, is likely to be the C_{12}–C_{13} stretch of isoiodopsin. The shoulder at ~1205 cm^{-1} is assigned to the degenerate C_{14}–C_{15} and C_8–C_9 stretches in correspondence with isorhodopsin. The prominent band at 1270 cm^{-1} in rhodopsin is the HC_{11}=$C_{12}H$ in-plane rocking mode that is characteristic of the 11-*cis* isomer (Curry et al., 1985; Palings et al., 1987). Because there is no peak that belongs to the 9-*cis* species in this region, the HC_{11}=$C_{12}H$ rock of iodopsin is assigned at ~1266 cm^{-1}. The rocking mode in isorhodopsin that is characteristic of the 9-*cis* geometry is the C_8H rock at ~1320 cm^{-1} (Curry et al., 1985). This mode is assigned at 1324 cm^{-1} in isoiodopsin.

The hydrogen out-of-plane (HOOP) wagging modes of the C_7=C_8 and C_{11}=C_{12} groups have frequencies near ~970 cm^{-1} (Eyring et al., 1982). In rhodopsin, the intense HC_{11}=$C_{12}H$ A_2 HOOP combination appears at 971 cm^{-1}. In isorhodopsin, the mode at 961 cm^{-1} is the HC_7=C_8H A_u HOOP vibration. The spectrum in Figure 3C contains corresponding lines at 960 and 970 cm^{-1} that are assigned to the HC_7=C_8H and HC_{11}=$C_{12}H$ HOOP modes of isoiodopsin and iodopsin, respectively. In addition, a new line is detected nearby at 976 cm^{-1}. Its frequency suggests that this mode may represent another HOOP vibration belonging to either iodopsin or isoiodopsin that has gained intensity, although it may also arise through a Fermi resonance with another weaker mode.

An expanded view of the Schiff base region of the iodopsin+isoiodopsin mixture in H_2O and D_2O is presented in Figure 4. The shoulder at 1644 cm^{-1} shifts down to 1621 cm^{-1} after the protein is suspended in a D_2O buffer. Therefore, the protonated Schiff base (C=NH) stretching mode is assigned at 1644 cm^{-1}. Most of the band intensity is attributed to iodopsin because it is the major component in the mixture. The 1631-cm^{-1} peak adjacent to the C=NH band is assigned to a localized C=C stretching mode and probably corresponds to the 1635-cm^{-1} mode observed in the spectra of rhodopsin and isorhodopsin.

Bathoiodopsin. The Raman spectra of bathoiodopsin and bovine bathorhodopsin are compared in Figure 5. The most intense bathoiodopsin mode is the in-phase C=C stretch at 1502 cm^{-1}. This mode is 34 cm^{-1} below the corresponding bathorhodopsin mode, indicating an extensive increase in electron delocalization. The fingerprint region of bathoiodopsin contains lines at 1145, 1180, 1212, and 1232 cm^{-1}. Bathorhodopsin modes are found at 1166, 1210, 1214, and 1240 cm^{-1}, which have been assigned to the C_{10}–C_{11}, C_{14}–C_{15}, C_8–C_9, and C_{12}–C_{13} stretches, respectively (Palings et al., 1989). The correspondence between the spectra of bathoiodopsin and bathorhodopsin is not as good as that seen for the

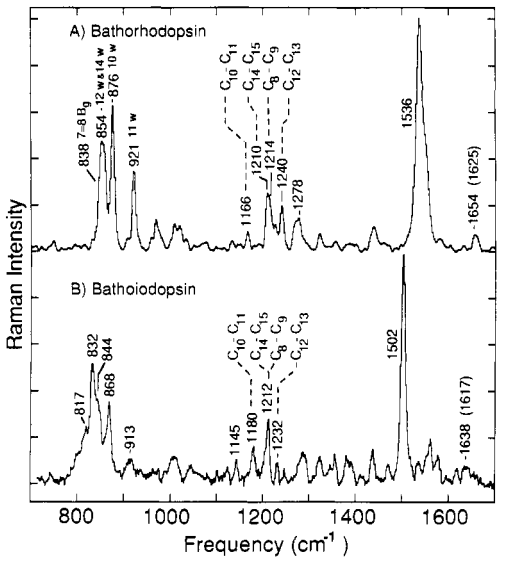

FIGURE 5: Resonance Raman spectra of (A) bathorhodopsin and (B) bathoiodopsin. The bathorhodopsin spectrum is reproduced from Palings et al. (1989). w = hydrogen wag vibration.

11-*cis* and 9-*cis* species of the chicken and bovine pigments. The simplest assumption, that the ordering of the C–C stretching modes is unchanged between the two batho species, requires the C_{10}–C_{11} stretch, which is usually found above 1160 cm^{-1} in retinals (Curry et al., 1985) and their protonated Schiff bases (Mathies et al., 1987), to be assigned at 1145 cm^{-1}. The C_{14}–C_{15} stretch would then be assigned at 1180 cm^{-1}, about 10 cm^{-1} lower than the typical frequency in retinal PSB molecules. These assignments are unlikely because we expect increased electron delocalization to result, if anything, in a general frequency upshift of the C–C modes. A more probable alternative (see Discussion) is to assign the 1180-cm^{-1} mode as the C_{10}–C_{11} stretch (Figure 5). The upshifted frequency is explained by a higher C–C bond order resulting from greater delocalization of the π-electron system in this red-shifted chromophore. The C_{14}–C_{15} stretch is then assigned at ~1212 cm^{-1}, nearly degenerate with the C_8–C_9 stretch. The C_{12}–C_{13} mode is assigned at 1232 cm^{-1}. The mode at 1145 cm^{-1} may then be one of the ionone ring vibrations that has picked up intensity (Curry et al., 1985).

The HOOP vibrations of bathorhodopsin consist of distinct lines at 875 and 921 cm^{-1}, and overlapping bands at 838, 850, and 858 cm^{-1} (Palings et al., 1989). The 921-cm^{-1} mode is an isolated $C_{11}H$ wag that is decoupled from the $C_{12}H$ wag because the $C_{12}H$ wag has shifted down to an unusually low frequency at 858 cm^{-1}. The 875-cm^{-1} mode consists of the $C_{10}H$ wag that is mixed with a $HC_7{=}C_8H$ B_g HOOP combination. The unresolved band at 838 cm^{-1} represents the $HC_7{=}C_8H$ B_g mode containing some $C_{10}H$ wag character. The $C_{14}H$ wag has been assigned at 850 cm^{-1}. The unusually strong intensities of these modes indicate a twisted chromophore structure in bathorhodopsin (Eyring et al., 1983; Warshel & Barboy, 1982).

The HOOP region of bathoiodopsin consists of strongly enhanced lines at 913, 868, 844, 832, and 817 cm^{-1}. Comparison with bathorhodopsin suggests that these modes are generally 10–20 cm^{-1} lower in frequency. On the basis of this correspondence, the $C_{11}H$ wag is assigned at 913 cm^{-1}. Its relative intensity is much weaker compared to the $C_{11}H$ wag of bathorhodopsin. The $C_{10}H$ wag is assigned to the next highest mode at 868 cm^{-1}. The shoulder at ~844 cm^{-1} is ascribed to the $C_{12}H$ wag, and the next intense mode at 832 cm^{-1} is assigned to the $C_{14}H$ wag.[2] The peak at 817 cm^{-1} probably corresponds to the $HC_7{=}C_8H$ B_g HOOP mode. The lower frequencies of these HOOP vibrations in bathoiodopsin may be due to the reduced π-bond order of the double bonds.

The C=N stretching mode of bathoiodopsin is assigned at 1638 cm^{-1} (Figure 4). When the nitrogen is deuterated, the band at ~1618 cm^{-1} doubles in intensity, and the 1638-cm^{-1} band disappears (Figure 4). This intensity increase is attributed to the C=N mode that has shifted down 21 cm^{-1} to 1617 cm^{-1} in D_2O.

DISCUSSION

The absorption maximum of a visual pigment is determined by the interaction of the 11-*cis*-retinal chromophore with its protein environment. The nature of the interactions can be elucidated by identifying perturbations imposed by the protein on the structure of the PSB chromophore and then assigning these perturbations to binding-site residues by performing, for example, Raman microscopy of site-specific mutants (Lin et al., 1992). Previous resonance Raman microprobe studies have examined the chromophore structures in visual pigments absorbing between 430 and 500 nm (Barry & Mathies, 1987). In particular, the mechanism of the opsin shift between blue- and green-sensitive pigments was investigated by comparing the Raman spectra of the green rod (λ_{max} ~430 nm) and red rod (λ_{max} ~502 nm) pigments from the toad *Bufo marinus* (Loppnow et al., 1989). The fingerprint regions of the green rod isorhodopsin and the 9-*cis*-retinal PSB in methanol were essentially identical, but the C=NH frequency of the green rod was 6 cm^{-1} higher. In contrast, the fingerprint region of the red rod isorhodopsin exhibited the same frequency upshift of the C_{10}–C_{11} and C_{14}–C_{15} stretches previously seen in bovine isorhodopsin, suggesting that the protein perturbations associated with these shifts may be involved in the mechanism of shifting the λ_{max} from 440 to ~500 nm. These data indicated that the 430-nm λ_{max} of the blue pigments is a result of a relatively unperturbed PSB chromophore located in a nonpolar binding site, that is experiencing stronger electrostatic interaction with its counterion.

In the present study, the mechanism of the opsin shift in red-sensitive (λ_{max} ~560 nm) visual pigments has been investigated by studying the chromophore structure of iodopsin, a red cone pigment from the chicken retina. Probe-only and pump+probe excitation of iodopsin at 77 K yields a pair of Raman spectra with different concentrations of iodopsin, isoiodopsin, and bathoiodopsin in the photostationary steady-state mixture. These spectra have been used to isolate a bathoiodopsin spectrum and an iodopsin spectrum containing some scattering from isoiodopsin. The HOOP, fingerprint, ethylenic, and Schiff base modes of iodopsin, isoiodopsin, and bathoiodopsin are assigned on the basis of changes in the pump/probe spectra and by comparison to analogous spectra of the bovine pigments. The vibrational spectra of iodopsin and its photoproducts can now be compared with those of other visual pigments to reveal changes in chromophore structure that are unique to this red-sensitive pigment.

Schiff Base Mode and Its Relation to the Opsin Shift. The most obvious difference between the Raman spectrum of iodopsin and bovine rhodopsin (Figure 3) occurs in the Schiff base stretching region. The C=NH mode of iodopsin is at

[2] The 832-cm^{-1} line is assigned to the $C_{14}H$ wag on the basis of the shift of this line in the Fourier transform infrared spectrum of iodopsin that has been regenerated with a 14-deuterioretinal derivative (Y. Shichida, unpublished results).

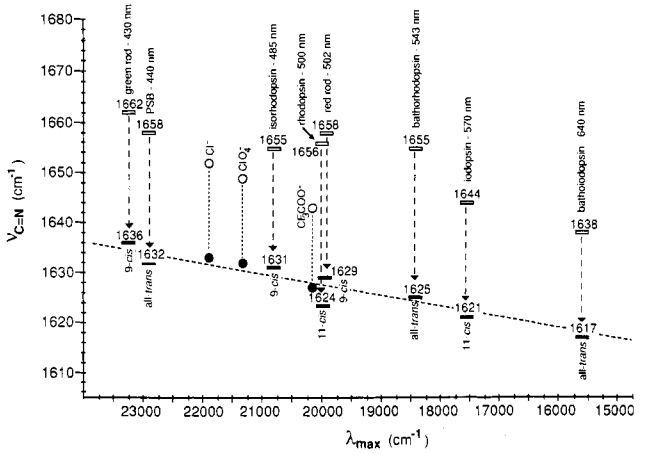

FIGURE 6: Frequencies of the C=NH (white bars) and C=ND (black bars) stretching modes from retinal PSB *n*-butylamine in methanol, toad green and red rods (Loppnow et al., 1989), rhodopsin, isorhodopsin, bathorhodopsin (Palings et al., 1987), iodopsin, and bathoiodopsin plotted against the absorption maxima of the pigments. The C=NH (○) and C=ND (●) frequencies of retinal PSB in CH_3Cl with the indicated counterion (Cl^-, ClO_4^-, CF_3COO^-) are also presented [data from Baasov et al. (1987)].

1644 cm^{-1}, ~12 cm^{-1} lower than the Schiff base frequency in rhodopsin and isorhodopsin. In D_2O, this mode shifts down to 1621 cm^{-1}, which is 3 cm^{-1} below that of rhodopsin. This 23-cm^{-1} D_2O shift is similar in magnitude to the shift seen in isorhodopsin, but considerably smaller than the ~33-cm^{-1} shift in rhodopsin. Because the C=NH stretching vibration is sensitive to the Schiff base environment (Baasov et al., 1987; Kakitani et al., 1985; Rodman Gilson et al., 1988), the lower C=N frequency in iodopsin provides structural evidence that the interactions between the protein and the PSB group of the 11-*cis* chromophores in iodopsin and rhodopsin are different.

In Figure 6, the frequencies of the C=N stretching modes of iodopsin, PSB model compounds, and the blue- and green-sensitive visual pigments are compared.[3] The plot shows that the C=NH mode follows a general trend toward lower frequency with longer wavelength. The C=NH frequency is highest for the blue pigment and decreases as the λ_{max} of the chromophore shifts toward the red, indicating that there is a change in the Schiff base structure that correlates with the opsin shift. However, among the bovine pigments and the toad red rod pigment which absorb between 485 and 540 nm, there is no clear correlation, and their C=NH frequencies are nearly identical and essentially unshifted from those of the model compounds (Deng & Callender, 1987; Palings et al., 1987) despite the large opsin shifts in these pigments.

To extract more specific structural conclusions about the Schiff base environment from the behavior of the C=NH stretching mode, we must first understand the factors that control its frequency. The C=NH frequency in retinals depends on three factors: (1) the intrinsic C=N bond order, (2) the coupling of the C=N stretch with the N–H rocking coordinate, and (3) possibly the coupling with nearby C=C stretching modes (Aton et al., 1980; Kakitani et al., 1983; Rodman Gilson et al., 1988; Smith et al., 1985, 1987b). Vibrational coupling between the C=C and C=N stretching coordinates results in a shift of the C=NH frequency if there is a corresponding shift of the C=C stretching frequency due to a change in the degree of π-electron delocalization. Because the delocalization is affected by environmental changes anywhere along the polyene, this coupling effect in principle can complicate the interpretation of the C=NH frequency shift. However, the shift due to C=C/C=N interaction is expected to be small because the two coordinates are only weakly coupled (Smith et al., 1985, 1987). Retinal analog studies confirm that a charge perturbation located near the ionone ring, which shifts the C=C mode by ~15 cm^{-1} and the λ_{max} by ~1500 cm^{-1}, produces only a small ~2-cm^{-1} shift of the C=NH mode (Baasov et al., 1987; Baasov & Sheves, 1985). Therefore, the Schiff base frequency in retinals is primarily sensitive to the C=N bond order and the C=NH rock–stretch coupling. Hydrogen bonding between the Schiff base N–H group and its environment affects the magnitude of the C=NH rock–stretch coupling because it modulates the N–H rock frequency. The effect of the rock–stretch coupling can be removed by deuterating the nitrogen so that the N–D rock is vibrationally decoupled from the C=N stretch because of its lower frequency. The difference in frequency between the protonated and deuterated Schiff base modes reflects the magnitude of this coupling and the strength of the hydrogen bonding. This suggests that the deuterated Schiff base (C=ND) frequency depends mostly on the C=N bond order. Model compound data (Baasov et al., 1987; Livnah & Sheves, 1993) indicate that a decrease of the C=ND frequency is correlated with enhanced delocalization caused by a positive charge positioned near the Schiff base or by a weaker electrostatic interaction between the PSB group and the counterion. In summary, the separability of the bond order and hydrogen-bonding effects on the C=N stretching mode should allow us to differentiate between changes in the electrostatic and hydrogen-bonding interactions of the Schiff base based on comparison of C=NH and C=ND frequencies.

When the C=ND frequencies of the pigments are compared, we see a clearer and more consistent inverse correlation with λ_{max}. The C=ND mode at 1636 cm^{-1} in the green rod shifts down to 1631 cm^{-1} in isorhodopsin and to 1629 cm^{-1} in the red rod. Rhodopsin has a very low C=ND mode at ~1624 cm^{-1} which shifts down by 2 cm^{-1} in iodopsin. The downshift from bathorhodopsin to bathoiodopsin is ~8 cm^{-1}. Because the C=ND frequency is mostly sensitive to the alteration of the electrostatic environment at the Schiff base, *the observed trend in the C=ND modes indicates that the reduction of the electrostatic interaction between the PSB group and its counterion is one way by which the visual pigments control their* λ_{max}. This conclusion is strongly supported by data on the C=ND frequencies of retinal PSB compounds in CH_3Cl which interact with the progressively more delocalized counterions Cl^-, ClO_4^-, and CF_3COO^- (see Figure 6). The slope of the line through these three C=ND frequencies is nearly the same as that for the pigments, demonstrating that the alteration of just the PSB–counterion interaction is simultaneously capable of accounting for the shifts in λ_{max} and the C=ND frequency. Furthermore, NMR model compound studies by Albeck and co-workers (Albeck et al., 1992) show that the ^{13}C chemical shifts of the chromophore in rhodopsin measured by Smith and co-workers (Smith et al., 1990) are consistent with a weak PSB–counterion interaction compared to that in the retinal PSB–chloride complex. Modeling of the NMR (Han et al., 1993) and two-photon absorption (Birge et al., 1988) data of rhodopsin with semiempirical molecular orbital calculations also suggests that the counterion interacts primarily with the C_{12}-to-C_{13} region

[3] The C=NH mode of a PSB model compound stabilized by a chloride ion in a leveling solvent such as ethanol is at ~1656 cm^{-1}. This frequency is the same in the *all-trans*, 11-*cis*, and 9-*cis* isomers (Mathies et al., 1977), indicating that this coordinate is localized and insensitive to the geometry of these polyenes. This suggests that we may compare the C=N mode of molecules that have different *cis–trans* configurations.

of the polyene instead of with the PSB group. The large D_2O shifts in the visual pigments are thought to be due to strong hydrogen bonding of the Schiff base nitrogen to a dipolar group such as water in the binding site (Han et al., 1993; Birge et al., 1988; Rafferty & Shichi, 1981). A recent model compound study has shown that the seemingly incompatible properties of red-shifted λ_{max} and the high C=NH and low C=ND frequencies can be mimicked in retinal analogs in which the PSB group interacts weakly with the counterion, but is hydrogen bonded to a separate dipolar group (Livnah & Sheves, 1993). Thus, the lack of a correlation in C=NH frequencies between some of the pigments is attributed to varying strengths of hydrogen bonding between the Schiff base and its hydrogen-bond acceptor in those pigments.

In bovine rhodopsin, the counterion is Glu-113 (Lin et al., 1992; Nathans, 1990a; Sakmar et al., 1989; Zhukovsky & Oprian, 1989). The PSB counterion in the vertebrate visual pigments is also thought to be the carboxylate group of a glutamic acid that is conserved in their amino acid sequences (Yoshizawa, 1992). In iodopsin, the glutamic acid is at position 126 (Kuwata et al., 1990; Tokunaga et al., 1990). The low C=ND frequency in iodopsin therefore indicates that the electrostatic interaction between the PSB group and Glu-126 is weaker. Increased separation between Glu-126 and the Schiff base moiety is one way this weaker interaction may be achieved. On the basis of analysis of the chromophore–counterion complex by Birge et al. (1985), the change required is small (<1 Å) because the electronic transition of retinal is extremely sensitive to the counterion location. Alternatively, the interaction can be weakened indirectly by a higher dielectric environment around the PSB group (Blatz & Mohler, 1972). Increases in the dielectric constant can be caused by the presence of more polar or polarizable residues, or more water molecules near Glu-126 in the binding site of iodopsin. It has been suggested that there is a hydrophilic pocket in iodopsin near helix 7 because the Schiff base and the protein are more susceptible to cleavage by hydroxylamine and chymotrypsin, respectively (Kuwata et al., 1990).

In bathoiodopsin, the interaction of the Schiff base with its counterion is much weaker, as indicated by its extremely low C=NH and C=ND frequencies (Figure 6). The lower C=ND frequency of bathoiodopsin compared to that of iodopsin shows that the interaction between the PSB group and its counterion environment becomes weaker after isomerization around the C_{11}=C_{12} bond. This reduction most likely contributes to the red-shift of the λ_{max} in this intermediate. This behavior contrasts with that seen in the bovine pigment in which rhodopsin and bathorhodopsin have C=NH and C=ND frequencies that differ by no more than 2 cm^{-1} (Eyring & Mathies, 1979; Palings et al., 1987). In rhodopsin, this observation suggests there is only a small change in the PSB–counterion interaction after isomerization. This has been rationalized by positioning the carboxylate counterion adjacent to the retinal molecular plane near C_{13} in the binding-site model of Birge et al. (1988).

Fingerprint Modes and Their Relation to the Opsin Shift. The C–C stretching modes of iodopsin are compared to those of rhodopsin and the 11-*cis* PSB model compound in Figure 7 to determine if there are additional perturbations that may be correlated with the opsin shift to 570 nm. In iodopsin, the C_{10}–C_{11} mode is shifted up to 1105 cm^{-1}, most likely due to higher bond order resulting from greater delocalization of the π-system caused by weaker electrostatic interaction between the counterion and the Schiff base moiety in this red-absorbing chromophore. The C_{14}–C_{15} stretch frequency is unchanged,

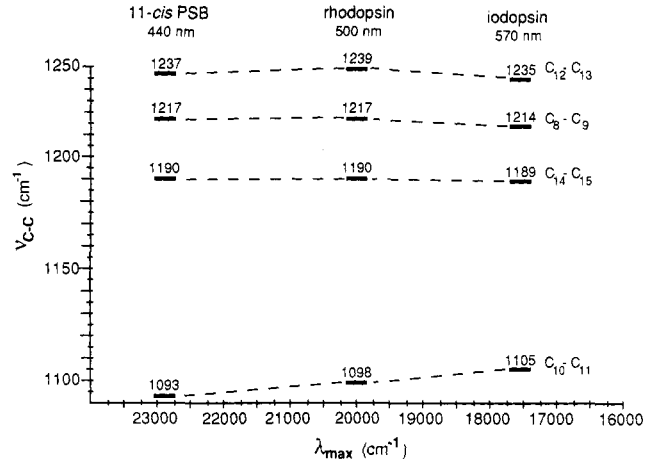

FIGURE 7: Fingerprint correlation diagram for 11-*cis*-retinal PSB *n*-butylamine, rhodopsin (Palings et al., 1987), and iodopsin.

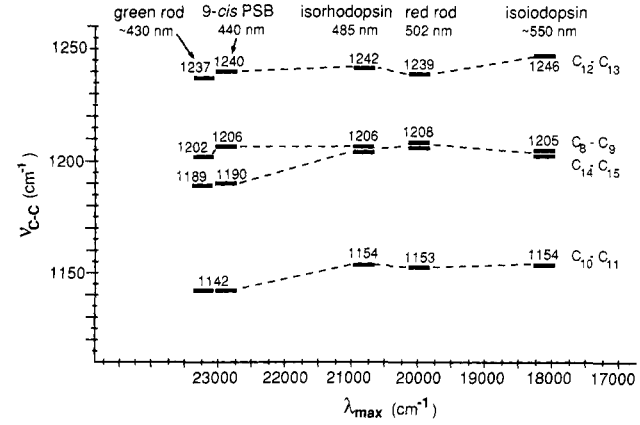

FIGURE 8: Fingerprint correlation diagram for 9-*cis*-retinal PSB *n*-butylamine, toad green and red rods (Loppnow et al., 1989), isorhodopsin (Palings et al., 1987), and isoiodopsin.

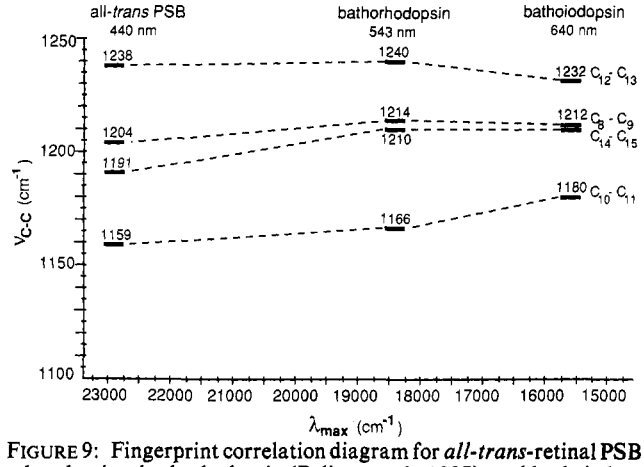

FIGURE 9: Fingerprint correlation diagram for *all-trans*-retinal PSB *n*-butylamine, bathorhodopsin (Palings et al., 1987), and bathoiodopsin.

but the C_8–C_9 and the C_{12}–C_{13} stretches are shifted down by ~3 cm^{-1} in iodopsin compared to rhodopsin. Similarly, the C–C stretching modes of isoiodopsin are basically at the same frequency as those of isorhodopsin and the red rod (Figure 8). These data show that the perturbation that causes the frequency shifts of the C–C modes in isorhodopsin and the red rod is not altered in isoiodopsin. *In general, the absence of any unusual frequency shifts of the C–C stretches of iodopsin and isoiodopsin argues that there are no new local protein perturbations associated with the opsin shift from 500 to 570 nm that perturb the ground-state chromophore*

structure. This result is consistent with the conclusion from analog regeneration experiments that the steric and electrostatic environments around the skeletal portion of the chromophore in the binding pockets of rhodopsin and iodopsin are similar (Fukada et al., 1990). Consequently, it is unlikely that there is a new protein charge perturbation near the center of the polyene chain in iodopsin that red-shifts the λ_{max}. In support of this view, the primary sequence of iodopsin does not contain more glutamic or aspartic residues in the transmembrane regions compared to rhodopsin (Kuwata et al., 1990).

Two possible assignments for the C–C stretches of bathoiodopsin have been presented under Results. We prefer the assignment of the C_{10}–C_{11} stretch at 1180 cm^{-1}. The C_{14}–C_{15} and C_8–C_9 stretches are then at about the same frequencies as in bathorhodopsin, whereas the C_{12}–C_{13} stretch has dropped down ~8 cm^{-1} to 1232 cm^{-1}. The C_{10}–C_{11} mode is shifted up ~14 cm^{-1} from the frequency in bathorhodopsin mainly because of increased bond order caused by increased electron delocalization. Vibrational analysis using the force fields of the *all-trans*-retinal PSB and the BR_{568} chromophore (Smith et al., 1985, 1987b) suggests that enhanced delocalization also alters the potential force constants involving couplings among the C=C and C–C stretching coordinates to decrease the C–C frequencies by a few wavenumbers. Because bathoiodopsin absorbs further to the red of BR_{568}, this coupling is expected to downshift the C–C stretches, and may be the reason for the lower C_{12}–C_{13} frequency.

HOOP Modes and Chromophore Structure. In bathoiodopsin, the relative intensities of the lines assigned to the $C_{11}H$ and $C_{10}H$ wags are weaker compared to those in bathorhodopsin, whereas the $C_{14}H$ wag intensity is stronger. Because HOOP vibrations in retinal polyenes are localized (Curry et al., 1985), this intensity pattern indicates that the chromophore structure is more distorted toward the Schiff base end in bathoiodopsin. This suggests that the opsin moiety has not yet relaxed sterically to accommodate the twisted *all-trans* chromophore to the same degree as in bathorhodopsin. The higher energy state of bathoiodopsin is also evident from the fact that while bathorhodopsin decays thermally to lumirhodopsin, bathoiodopsin is unable to relax to the lumi state and converts back to iodopsin (Imamoto et al., 1989).

In contrast to bathoiodopsin, the HOOP vibrations of iodopsin and isoiodopsin are less perturbed. The characteristic HOOP lines for 11-*cis*- and 9-*cis*-retinals (Curry et al., 1985; Palings et al., 1987) are observed at 970 and 960 cm^{-1}, respectively. In general, the correspondence of the HOOP regions of iodopsin and rhodopsin supports the earlier conclusion regarding the similarity of the protein environments in the ground states of the chicken and bovine pigments.

CONCLUSIONS

The resonance Raman spectra of iodopsin exhibit spectral features that report on alterations of the protein–chromophore interactions in the red-sensitive visual pigments. The low C=ND frequency in iodopsin shows that the opsin shift of the λ_{max} to a longer wavelength (570 nm) is accompanied by a weaker electrostatic interaction between the PSB group and its counterion. The C=ND modes of the various pigments characterized to date also display a consistent decrease in frequency with increasing wavelength of the pigment λ_{max}, indicating that *the modulation of the PSB–counterion interaction is an important mechanism by which the protein tunes the λ_{max} from 430 to 570 nm.*

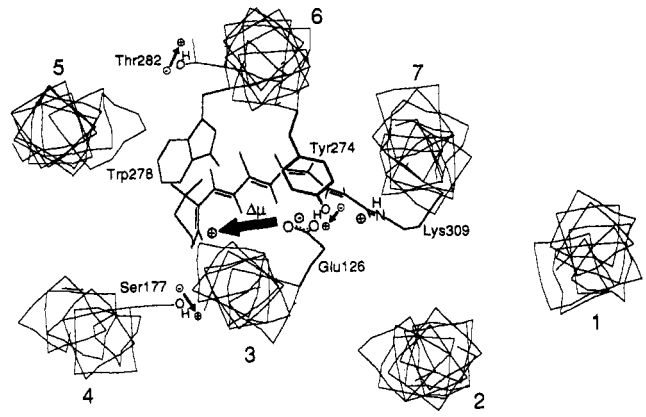

FIGURE 10: Model for the retinal binding site in iodopsin illustrating the mechanism of the opsin shift in red visual pigments. The seven α-helices were positioned on the basis of the two-dimensional projection map of rhodopsin (Schertler et al., 1993), and their faces were oriented according to the model of rhodopsin and G-protein-coupled receptors (Baldwin, 1993). The directions of the dipole moments (μ) on the residues are indicated by arrows. Optical excitation of the retinyl cation is accompanied by a large shift of positive charge density from the Schiff base toward the ionone ring that increases the dipole moment ($\Delta\mu$ ~10 D) (Mathies & Stryer, 1976). Ser-177 and Thr-282 contribute to the red-shift because these dipolar residues stabilize the excited-state dipolar charge distribution more than the ground-state distribution. Tyr-274 contributes to the opsin shift by dielectrically stabilizing the PSB group and its counterion, thereby reducing the strength of the electrostatic interaction between the retinyl cation and the carboxylate anion.

The absorption maxima of iodopsin and the human red cone pigment are shifted ~1000 cm^{-1} to the red of the respective green cone pigments. From comparison of the sequences and the λ_{max} values of a number of primate visual pigments, Neitz and co-workers (Neitz et al., 1991) proposed that changing three residues from nonpolar to polar amino acids can account for the opsin shift between the green and red cone pigments. In the human red pigment, the three polar residues are Ser-180, Tyr-277, and Thr-285; the corresponding residues in iodopsin are Ser-177, Tyr-274, and Thr-282 (Yoshizawa & Kuwata, 1991). Because the changes all involve the net gain of polar groups, the opsin shift most likely originates from the electrostatic interaction between these dipolar side chains and the chromophore. The transition from the ground electronic state to the first excited state in a retinal PSB chromophore is characterized by a migration of positive charge density from the PSB moiety toward the ionone ring that results in a dramatic increase of the excited-state dipole moment. For example, in the *all-trans*-retinal PSB, the increase is as large as ~12 D in the first excited state (Mathies & Stryer, 1976). Sheves and co-workers (Baasov et al., 1987; Baasov & Sheves, 1985) have shown that a nonconjugated positive charge located near the ring and/or the C_9-position shifts the λ_{max} of the PSB molecule to a bluer wavelength, whereas a positive charge near the Schiff base red-shifts the λ_{max}. Negative charges at these locations induce shifts in the opposite directions. The direction of these shifts can be explained by the interaction of these charges with the change in the charge distribution of retinal upon excitation. Because of the increase in positive charge density near the ionone ring in the excited state, *a negative charge (or the negative end of a dipole) close to the ring will preferentially stabilize the energy of the excited state relative to that of the ground state, thereby inducing a red-shift of the absorption band.*

A model that uses protein dipoles to explain the opsin shift in iodopsin is presented in Figure 10. If we make the assumption that the tertiary structures of iodopsin and

rhodopsin are similar, then Tyr-274 is expected to reside near the PSB region, and Ser-177 and Thr-282 would be positioned in the vicinity of the ionone ring. The dipoles of Ser-177 and Thr-282 are oriented so that they will perferentially stabilize the excited-state charge distribution and induce a red-shift of the λ_{max}. Tyr-274 also contributes to the red-shift by orienting its dipole to stabilize the PSB ion pair, thereby weakening the PSB–counterion electrostatic interaction. Sakmar and coworkers (Chan et al., 1992) have examined the individual effects of these dipolar residues on the pigment λ_{max} by mutating the homologous nonpolar residue (Ala-164, Phe-261, and Ala-269) in bovine rhodopsin to the corresponding polar residue (Ser, Tyr, or Thr) found in the red pigments. They found that Ser, Tyr, and Thr can individually induce red-shifts of $\sim$100, 400, and 500 cm^{-1}, respectively. Therefore, most of the opsin shift between the green and the red cone pigments can be assigned to the presence of the three hydroxyl-bearing residues. The downshift of the C=N mode of iodopsin is consistent with the idea that a dipolar residue such as Tyr-274 decreases the strength of the interaction between the PSB group and the counterion environment. Furthermore, the absence of any unusual changes in the C–C stretching modes indicates that the opsin shift in iodopsin is not caused by the addition or shift of a charged residue along the polyene. *We conclude that the opsin shift in red visual pigments is achieved by increasing the dipolar dielectric properties of the retinal binding pocket to stabilize (i.e., reduce) the electrostatic interaction between the Schiff base and the counterion, and to differentially stabilize the dipolar excited state of the retinal chromophore.*

REFERENCES

Albeck, A., Livnah, N., Gottlieb, H., & Sheves, M. (1992) *J. Am. Chem. Soc. 114*, 2400–2411.

Aton, B., Doukas, A. G., Narva, D., Callender, R. H., Dinur, U., & Honig, B. (1980) *Biophys. J. 29*, 79–94.

Baasov, T., & Sheves, M. (1985) *J. Am. Chem. Soc. 107*, 7524–7533.

Baasov, T., Friedman, N., & Sheves, M. (1987) *Biochemistry 26*, 3210–3217.

Baldwin, J. M. (1993) *EMBO J. 12*, 1693–1703.

Barry, B., & Mathies, R. A. (1987) *Biochemistry 26*, 59–64.

Birge, R. R., Murray, L. P., Pierce, B. M., Akita, H., Balogh-Nair, V., Findsen, L. A., & Nakanishi, K. (1985) *Proc. Natl. Acad. Sci. U.S.A. 82*, 4117–4121.

Birge, R. R., Einterz, C. M., Knapp, H. M., & Murray, L. P. (1988) *Biophys. J. 53*, 367–385.

Blatz, P. E., & Mohler, J. H. (1972) *Biochemistry 11*, 3240–3243.

Blatz, P. E., Mohler, J. H., & Navangul, H. V. (1972) *Biochemistry 11*, 848–855.

Chan, T., Lee, M., & Sakmar, T. P. (1992) *J. Biol. Chem. 267*, 9478–9480.

Chen, J. G., Nakamura, T., Ebrey, T. G., Ok, H., Konno, K., Derguini, F., Nakanishi, K., & Honig, B. (1989) *Biophys. J. 55*, 725–729.

Curry, B., Palings, I., Broek, A. D., Pardoen, J. A., Lugtenburg, J., & Mathies, R. (1985) *Adv. Infrared Raman Spectrosc. 12*, 115–178.

Deng, H., & Callender, R. H. (1987) *Biochemistry 26*, 7418–7426.

Doukas, A. G., Aton, B., Callender, R. H., & Ebrey, T. G. (1978) *Biochemistry 17*, 2430–2435.

Eyring, G., & Mathies, R. (1979) *Proc. Natl. Acad.* Sci. *U.S.A. 76*, 33–37.

Eyring, G., Curry, B., Broek, A., Lugtenburg, J., & Mathies, R. (1982) *Biochemistry 21*, 384–393.

Fukada, Y., Okano, T., Shichida, Y., Yoshizawa, T., Trehan, A., Mead, D., Denny, M., Asato, A. E., & Liu, R. S. H. (1990) *Biochemistry 29*, 3313–3140.

Han, M., DeDecker, B. S., & Smith, S. O. (1993) *Biophys. J. 65*, 899–906.

Harbison, G. S., Smith, S. O., Pardoen, J. A., Courtin, J. M. L., Lugtenburg, J., Herzfeld, J., Mathies, R. A., & Griffin, R. G. (1985) *Biochemistry 24*, 6955–6962.

Honig, B., Greenberg, A. D., Dinur, U., & Ebrey, T. G. (1976) *Biochemistry 15*, 4593–4599.

Honig, B., Dinur, U., Nakanishi, K., Balogh-Nair, V., Gawinowicz, M. A., Arnaboldi, M., & Motto, M. G. (1979) *J. Am. Chem. Soc. 101*, 7084–7086.

Hubbard, R., & Kropf, A. (1959) *Nature 183*, 448–450.

Imamoto, Y., Kandori, H., Okano, T., Fukada, Y., Shichida, Y., & Yoshizawa, T. (1989) *Biochemistry 28*, 9412–9416.

Irving, C. S., Byers, G. W., & Leermakers, P. A. (1970) *Biochemistry 9*, 858–864.

Kakitani, H., Kakitani, T., Rodman, H., Honig, B., & Callender, R. (1983) *J. Phys. Chem. 87*, 3620–3628.

Kakitani, H., Kakitani, T., Rodman, H., & Honig, B. (1985) *Photochem. Photobiol. 41*, 471–479.

Kandori, H., Mizukami, T., Okada, T., Imamoto, Y., Fukada, Y., Shichida, Y., & Yoshizawa, T. (1990) *Proc. Natl. Acad. Sci. U.S.A. 87*, 8908–8912.

Kleinschmidt, J., & Harosi, F. I. (1992) *Proc. Natl. Acad. Sci. U.S.A. 89*, 9181–9185.

Kuwata, O., Imamoto, Y., Okano, T., Kokame, K., Kojima, D., Matsumoto, H., Morodome, A., Fukada, Y., Shichida, Y., Yasuda, K., Shimura, Y., & Yoshizawa, T. (1990) *FEBS Lett. 272*, 128–132.

Lin, S. W., Sakmar, T. P., Franke, R. R., Khorana, H. G., & Mathies, R. A. (1992) *Biochemistry 31*, 5105–5111.

Livnah, N., & Sheves, M. (1993) *J. Am. Chem. Soc. 115*, 351–353.

Loppnow, G. R., & Mathies, R. A. (1989) *Rev. Sci. Instrum. 60*, 2628–2630.

Loppnow, G. R., Barry, B. A., & Mathies, R. A. (1989) *Proc. Natl. Acad. Sci. U.S.A. 86*, 1515–1518.

Lythgoe, J. N. (1972) *Handbook of Sensory Physiology* (Dartnall, H. J. A., Ed.) pp 604–624, Springer-Verlag, New York.

Makino, C. L., Kraft, T. W., Mathies, R. A., Lugtenburg, J., Miley, M. E., van der Steen, R., & Baylor, D. A. (1990) *J. Physiol. 424*, 545–560.

Mathies, R., & Stryer, L. (1976) *Proc. Natl. Acad. Sci. U.S.A. 73*, 2169–2173.

Mathies, R., & Yu, N.-T. (1978) *J. Raman Spectrosc. 7*, 349–352.

Mathies, R., Oseroff, A. R., & Stryer, L. (1976) *Proc. Natl. Acad. Sci. U.S.A. 73*, 1–5.

Mathies, R., Freedman, T. B., & Stryer, L. (1977) *J. Mol. Biol. 109*, 367–372.

Mathies, R. A., Smith, S. O., & Palings, I. (1987) *Biological Applications of Raman Spectroscopy* (Spiro, T. G., Ed.) Vol. 2, pp 59–108, John Wiley and Sons, Inc., New York.

Nakanishi, K., Balogh-Nair, V., Arnaboldi, M., Tsujimoto, K., & Honig, B. (1980) *J. Am. Chem. Soc. 102*, 7945–7947.

Nathans, J. (1990a) *Biochemistry 29*, 9746–9752.

Nathans, J. (1990b) *Biochemistry 29*, 937–942.

Neitz, M., Neitz, J., & Jacobs, G. H. (1991) *Science 252*, 971–974.

Okano, T., Fukada, Y., Artamonov, I. D., & Yoshizawa, T. (1989) *Biochemistry 28*, 8848–8856.

Palings, I., Pardoen, J. A., van den Berg, E., Winkel, C., Lugtenburg, J., & Mathies, R. A. (1987) *Biochemistry 26*, 2544–2556.

Palings, I., van den Berg, E. M. M., Lugtenburg, J., & Mathies, R. A. (1989) *Biochemistry 28*, 1498–1507.

Rafferty, C. N., & Shichi, H. (1981) *Photochem. Photobiol. 33*, 229–234.
Rimai, L., Heyde, M. E., & Gill, D. (1973) *J. Am. Chem. Soc. 95*, 4493–4501.
Rodman Gilson, H. S., Honig, B. H., Croteau, A., Zarrilli, G., & Nakanishi, K. (1988) *Biophys. J. 53*, 261–269.
Sakmar, T. P., Franke, R. R., & Khorana, H. G. (1989) *Proc. Natl. Acad. Sci. U.S.A. 86*, 8309–8313.
Schertler, G. F. X., Villa, C., & Henderson, R. (1993) *Nature 362*, 770–772.
Shichida, Y., Okada, T., Kandori, H., Fukada, Y., & Yoshizawa, T. (1993) *Biochemistry 32*, 10832–10838.
Smith, S. O., Myers, A. B., Mathies, R. A., Pardoen, J. A., Winkel, C., van den Berg, E. M. M., & Lugtenburg, J. (1985) *Biophys. J. 47*, 653–664.
Smith, S. O., Palings, I., Copié, V., Raleigh, D. P., Courtin, J., Pardoen, J. A., Lugtenburg, J., Mathies, R. A., & Griffin, R. G. (1987a) *Biochemistry 26*, 1606–1611.
Smith, S. O., Braiman, M. S., Myers, A. B., Pardoen, J. A., Courtin, J. M. L., Winkel, C., Lugtenburg, J., & Mathies, R. A. (1987b) *J. Am. Chem. Soc. 109*, 3108–3125.
Smith, S. O., Palings, I., Miley, M. E., Courtin, J., de Groot, H., Lugtenburg, J., Mathies, R. A., & Griffin, R. G. (1990) *Biochemistry 29*, 8158–8164.
Tokunaga, F., Iwasa, T., Miyagishi, M., & Kayada, S. (1990) *Biochem. Biophys. Res. Commun. 173*, 1212–1217.
Tsukamoto, Y., Horiuchi, S., & Yoshizawa, T. (1975) *Vision Res. 15*, 819–823.
van der Steen, R., Biesheuvel, P. L., Mathies, R. A., & Lugtenburg, J. (1986) *J. Am. Chem. Soc. 108*, 6410–6411.
Wang, Z., Asenjo, A. B., & Oprian, D. D. (1993) *Biochemistry 32*, 2125–2130.
Warshel, A., & Barboy, N. (1982) *J. Am. Chem. Soc. 104*, 1469–1476.
Yoshizawa, T. (1992) *Photochem. Photobiol. 56*, 859–867.
Yoshizawa, T., & Wald, G. (1963) *Nature 197*, 1279–1286.
Yoshizawa, T., & Wald, G. (1967) *Nature 214*, 566–571.
Yoshizawa, T., & Kuwata, O. (1991) *Photochem. Photobiol. 54*, 1061–1070.
Zhukovsky, E. A., & Oprian, D. D. (1989) *Science 246*, 928–930.